

Original Article

Cite this article: Mathuthu M, Mdziniso NW, Asres YH. (2019) Dosimetric evaluation of cobalt-60 teletherapy in advanced radiation oncology. *Journal of Radiotherapy in Practice* 18: 88–92. doi: 10.1017/S1460396918000390

Received: 8 June 2018

Revised: 1 August 2018

Accepted: 12 August 2018

First published online: 26 October 2018

Key words:

accelerator; cobalt-60; fluence; IMRT; teletherapy

Author for correspondence:

Yihunie Hibstie Asres, North West University (Mafikeng Campus), Private Bag X2046, Mmabatho 2735, South Africa.
E-mail: yihuniehibs@gmail.com

Dosimetric evaluation of cobalt-60 teletherapy in advanced radiation oncology

Manny Mathuthu, Nhlakanipho Wisdom Mdziniso and Yihunie Hibstie Asres

Center for Applied Radiation Science and Technology, North West University (Mafikeng), Mmabatho, South Africa

Abstract

Background: Recent investigations demonstrate a strong potential for cobalt-60 (Co-60)-based teletherapy. The influence of the lower energy and penetration of a cobalt-60 beam compared with linear accelerator beams is negligible for intensity-modulated radiotherapy. **Purpose:** The aim of this research is to investigate source head fluence modulation in cobalt-60 teletherapy by using a three-dimensional (3D) physical compensator and secondary collimator jaw motion. **Materials and methods:** The Oncentra treatment planning system was used to develop three hypothetical plans by secondary collimator jaw motion. A clinical MDS Nordion Equinox 80 cobalt-60 teletherapy unit was used to acquire conventional water phantom beam characteristics. Fluence modulation experiments were executed at 5.0 cm depth in a PTW universal intensity-modulated radiation therapy (IMRT) verification phantom using calibrated Gafchromic external beam therapy 2 (EBT2) and RTQA2-1010 film batches. Gafchromic EBT2 film was used to sample intensity maps generated by secondary collimator jaw motion, yet Gafchromic RTQA2-1010 film sampled maps from the 3D physical compensator. The solid-state drives used were 75.0 and 74.3 cm for the Gafchromic EBT2 and Gafchromic RTQA2-1010 film measurements. **Results:** A 2D gamma index analysis was coded to compare EBT2 film measurements with Digital Imaging and Communications in Medicine data. This analysis was also used to verify film measurements versus Monte-Carlo simulations. **Conclusion:** Lateral beam profiles generated from water phantom measurements were used to establish source head fluence modulation on the film measurements. The source head fluence of a cobalt-60 teletherapy beam could be modulated by secondary collimator jaw motion and using a 3D physical compensator.

Introduction

Cobalt-60 teletherapy units and linear accelerator systems (linacs)^{1–3} were introduced nearly simultaneously in the early 1950s and emerged as rival technologies for external beam therapy. The potential of Co-60 teletherapy in advanced radiation oncology mode with Monte-Carlo (MC)^{1,3} dose planning and verification has not been probed for the past few decades, even though it may offer similar advantages as linear accelerators.^{4–6} A few advanced radiation treatment planning studies have been done for Co-60 teletherapy,⁷ although this modality involves a high-energy photon beam.^{3,6–8} Intensity-modulated radiation therapy (IMRT) with Co-60 teletherapy^{9,10} can be suitable for complex superficial anatomic sites, and it can minimise the incidence of radiation toxicity in proximal organ at risk volume.^{11,12} Integrating technologies like multileaf collimator in Co-60 teletherapy^{1,3,7} units can facilitate automated treatment.^{1,2,4,13} It is therefore important for medical physicists to consider the role of Co-60 teletherapy in advanced technologies like IMRT.^{8,13,14} Co-60⁷ based radiation therapy continues to play a significant role in not only developing countries where access to radiation therapy is extremely limited but also in industrialised countries.^{9,10,15}

Many treatment planning systems do not effectively model the lateral beam degradation that occurs at depth with the small radiation beamlets from linear accelerator IMRT.^{16,17} These beamlets result in the loss of lateral electron equilibrium for the higher energy linear accelerator photon beams.^{16,17} The implementation of IMRT with Co-60 teletherapy units might mitigate this effect due to the wider beam penumbra and shorter ranges of secondary electrons at depth.^{3,16,17} Intensity-modulated Co-60 teletherapy beams are immune to the neutron contamination characteristic of photon energies ≥ 8 MeV.^{14,16} The smaller sizes of current IMRT beamlets pose a greater uncertainty in the accuracy of clinical dosimetry owing to the lack of charged particle equilibrium conditions at depth.^{17,18} IMRT with Co-60 teletherapy beams using modern MC dose planning therefore might yield greater dosimetric

© Cambridge University Press 2018.
This is an Open Access article, distributed under the terms of the Creative Commons Attribution licence (<http://creativecommons.org/licenses/by/4.0/>), which permits unrestricted re-use, distribution, and reproduction in any medium, provided the original work is properly cited.

CAMBRIDGE
UNIVERSITY PRESS

accuracy.^{7,17} MC simulations were used to calculate the percentage depth dose (PDD) and profile data for pencil beams (or beamlets) that could be then combined to produce fan beam intensity modulation.^{1,4}

Materials and Methods

Equipment used

Measurements were carried out on a clinical MDS Nordion Equinox 80 Co-60 teletherapy unit (Ontario, Canada)⁷ at Charlotte Maxeke Johannesburg Academic Hospital. This unit had a 1.5 cm diameter source delivering an output of $67.7 \text{ cGy/min} \pm 5.0\%$ in a $10 \text{ cm} \times 10 \text{ cm}$ square field at 80 cm source-to-axis distance (SAD) at the depth of maximum dose on the 1 September 2015. Figure 1 shows a picture of this Co-60 teletherapy machine.

A 0.125 cc PTW 31010 semi-flex thimble chamber and a TANDEM dual-channel electrometer (PTW, Freiburg, Germany) that had been interfaced with the PTW MEPHYSTO (Medical Physics Tool) software were used for central-axis depth dose and off-axis ratio measurements in a PTW MP3 phantom (PTW, Freiburg, Germany)¹⁹ filled with deionised water. A calibrated Lufft OPUS 20 device was used to correct for changes in the thimble chamber's response with temperature and pressure. Figure 2 shows a picture of the PTW MP3 phantom tank beneath the Co-60 teletherapy source head.

The first set of fluence measurements was taken with Gafchromic external beam therapy (EBT2) film at 5.0 cm depth in a PTW universal IMRT verification phantom.¹⁹ The second set of fluence measurements was taken with Gafchromic RTQA2-1010 film²⁰ at 5 cm depth in the PTW universal IMRT verification phantom. Dose rate constancy checks were made with the 0.125 cc thimble chamber that was positioned along the beam central axis at 1.0 cm beneath the film plane. A PTW Unidose E electrometer (10001) was used. Additional acrylic slabs were used with the IMRT phantom for backscatter, and a 5.0 cm thick acrylic layer was used for build-up. Figure 3 shows the geometric setup that was used for the film dosimetry measurements.^{21–23}

A physical compensator was manually designed and constructed to yield five intensity levels, and it comprised eight lead (Pb) strips that were affixed to a 6 mm thick acrylic accessory holding plate. Four different thicknesses of lead were used, and they were symmetrically positioned about the axial plane in the *x*-direction. A $2 \text{ cm} \times 10 \text{ cm}$ central gap was allowed to determine the transmission of the plate. A 1 mm thick $10 \text{ cm} \times 4 \text{ cm}$ lead strip, a 2 mm thick $10 \text{ cm} \times 3 \text{ cm}$ lead strip, a 3 mm thick

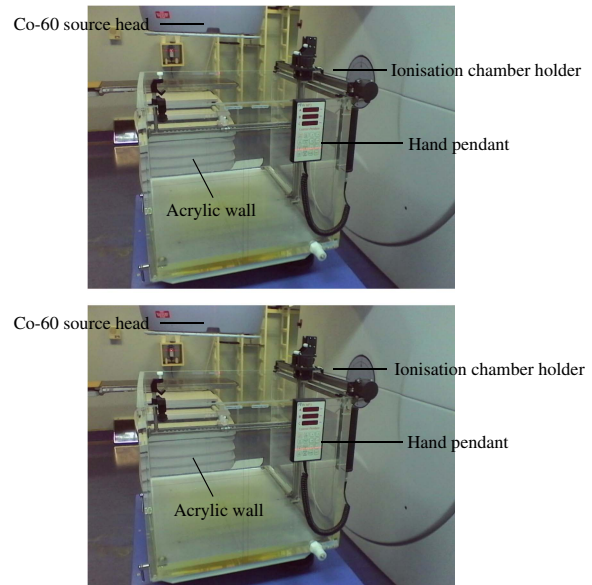


Figure 2. An automated PTW MP3 water phantom tank at Charlotte Maxeke Johannesburg Academic Hospital.

$10 \text{ cm} \times 2 \text{ cm}$ lead strip and a 5 mm thick $10 \text{ cm} \times 1 \text{ cm}$ lead strip were sequentially embedded one on top of another to achieve net thicknesses of 1, 3, 6 and 11 mm, respectively. Figure 4 is a coronal view of the physical compensator used in this study.

The second set of IMRT film dosimetry measurements was made with a three-dimensional (3D) physical compensator at the machine source head. They were initialised by calibrating a batch of Gafchromic RTQA2-1010 films to eight dose points that were in the range of 0–400 cGy, and more calibration points were sampled at lower doses. The same procedure used during the calibration of Gafchromic EBT2 film²⁰ for the first set of measurements was adhered to before exposure of film from the same batch in the presence of a 3D physical compensator at the machine source head.

With a gantry angle of zero, the physical compensator was placed in the accessory holder on a horizontal plane at a distance of about 56 cm from the source. Two sheets from the calibrated batch of Gafchromic RTQA2-1010 film were then exposed to prescribed isocentre doses of 104.3 and 203.0 cGy, consecutively, in a $14 \text{ cm} \times 14 \text{ cm}$ field that was symmetric about the axial and sagittal planes at 80 cm SAD. Two consecutive irradiations of the calibrated Gafchromic RTQA2-1010 films were made to deliver

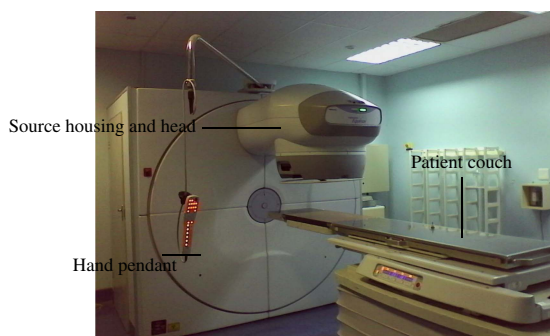


Figure 1. Clinical MDS Nordion Equinox 80 Co-60 teletherapy unit⁷ at Charlotte Maxeke Johannesburg Academic Hospital.

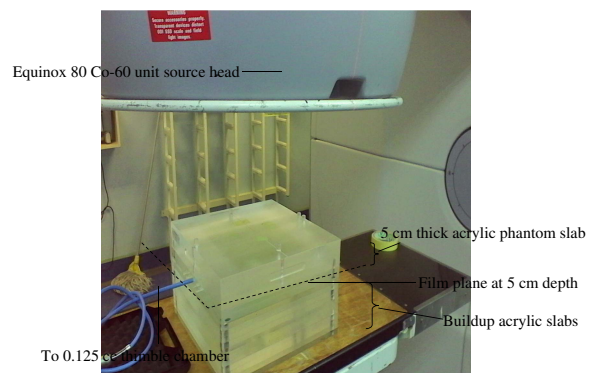


Figure 3. IMRT film dosimetry apparatus used at Charlotte Maxeke Johannesburg Academic Hospital.

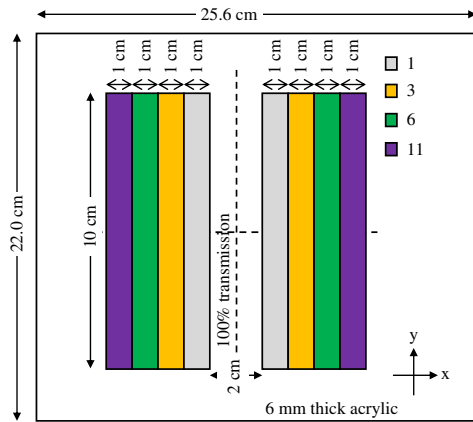


Figure 4. Coronal view of the three-dimensional physical compensator designed and used for the second set of measurements that were taken with Gafchromic RTQA2-1010 film.

the prescribed doses with a 14 cm × 14 cm symmetric field. A calibrated Lufft OPUS 20 device was used to monitor the treatment room temperature and pressure during both irradiation procedures. The films were handled, stored and processed in the same manner as in the first set of fluence measurements.

Water phantom measurements

PDD was measured at 70 cm solid-state drive (SSD) in field sizes of 5 cm × 5 cm, 10 cm × 10 cm, 15 cm × 15 cm and 20 cm × 20 cm, symmetric about the axial and sagittal planes. Scan data were normalised to the dose in a 10 cm × 10 cm field at 10 cm depth. PDD curves were then generated with Matrix Laboratory (MATLAB, Freiburg, Germany) from the MEPHYSTO file data. Off-axis ratios were measured by water phantom scans in symmetric field sizes of 5 cm × 5 cm, 10 cm × 10 cm, 15 cm × 15 cm and 20 cm × 20 cm. The off-axis data were normalised to the dose in a 10 cm × 10 cm field at 10 cm depth in water.

IMRT film dosimetry measurements

The first set of IMRT dosimetry measurements was initiated by calibrating Gafchromic EBT2 film at 5.0 cm depth in a PTW universal IMRT verification phantom (PTW, Freiburg, Germany).^{19,21,23} A single batch of 14 inch × 17 inch (35.6 cm × 43.2 cm) film was used. Two film sheets were cut into eight sub-strips and stored in the same box for uniformities in optical density (OD) response.²² One of the eight sub-strips was retained as an un-irradiated control. The other seven sub-strips were exposed in a 10 cm × 10 cm square field at 5.0 cm depth in the IMRT phantom to respective doses in the range of 5–330 cGy. A 0.125 cc PTW semi-flex thimble chamber was positioned along the beam central axis at 1.0 cm beneath the film plane to monitor for dose rate constancy. The IMRT phantom cross hairs were aligned with the treatment room laser lights, and each film sub-strip was marked and fixed to the phantom with tape to localise the isocentre. A calibrated Lufft OPUS 20 device was used for temperature, pressure and humidity readings, which were crucial for post-irradiation film dosimetry.^{22,24}

All eight sub-strips were properly handled with gloves to make sure that there was no fingerprint influence on OD_{net} , and it was stored for 48 hours in a radiation-free environment.^{22,24} Scan acquisitions were made in the film coating direction to minimise polarisation effects.²² Scans were acquired via the PTW FilmScan software, which was interfaced with the Epson Expression 10000 XL

flatbed colour scanner (Johannesburg, South Africa). The \overline{OD} value generated from the control film sub-strip served as a background reading (OD_b) that was deducted from every other nonzero dose point to deduce the corresponding OD_{net} . Subsequent film dosimetry measurements were then made relative to the calibration curve generated in this way.

IMRT by symmetric square jaw motions

Each input file used point detectors at several evenly spaced off-axis positions on the film plane in the IMRT verification phantom.^{19,22} Different simulation times were used for the different source diameters to facilitate the convergence of the detector tally scores. All input files were executed with Monte-Carlo N-Particle eXtended (MCNPX 2.7.0) to sample point-averaged photon fluxes at the various off-axis positions on the film plane. The corresponding OD_{net} values from Gafchromic EBT2 film measurements were normalised to the isocentre for the gamma index evaluation against the MCNPX tally output and Digital Imaging and Communications in Medicine (DICOM) printouts.

Co-60 IMRT by asymmetric rectangular jaw motions

Input files differed from the above case in terms of the symmetries of the secondary collimation's inclined planes about the axial and sagittal planes. Each input file employed point detectors at several evenly spaced off-axis positions on the film plane in the IMRT verification phantom.^{19,21–23} The same tactics as in previous two cases were used to facilitate the convergence of the detector tally scores.

Results and Discussions

Standard beam data

The conventional characteristics of the cobalt-60 beam were derived from central-axis and off-axis measurements in a water phantom. They were used as a reference to IMRT measurements with Gafchromic EBT2 and RTQA2-1010 films.

Percentage depth-dose data

Central-axis depth-dose depositions by several open beams exhibited a maximum dose deposition depth (D_{max}) of about 0.4–0.5 cm. The field size dependence of the magnitudes of the central-axis depth-dose depositions arises from collimator and in-phantom scatters. The curves were in agreement with the published relative dose data.¹³ Figure 5 is a plot of the central-axis depth ionisation curves for the four different field sizes measured in water.

Lateral beam profile data

Open-beam off-axis profiles for various field sizes at depth in water were obtained, and these compared well with published data.¹³ Furthermore, these served as a reference to the lateral beam profiles generated from film measurements and verified the feasibility of this study. Figure 6 is a plot of the lateral beam profiles that were generated for symmetric field sizes of 5 cm × 5 cm, 10 cm × 10 cm, 15 cm × 15 cm and 20 cm × 20 cm at 10 cm depth in a water phantom set to 70 cm SSD.

Intensity-modulated beam data

The feasibility of modulating the source head fluence of a cobalt-60 beam using a 3-D physical compensator and by secondary

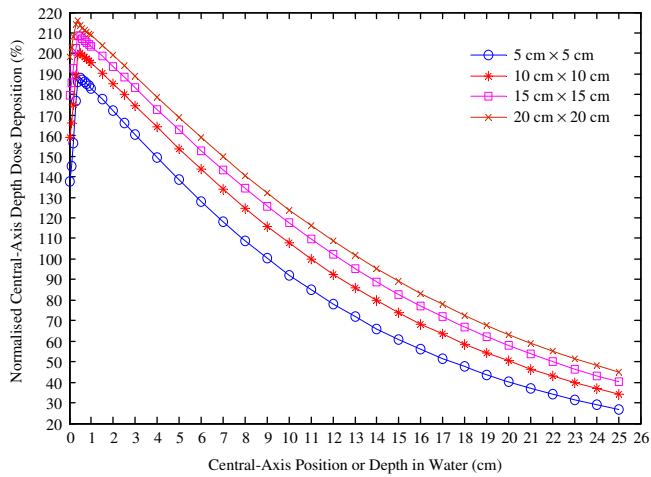


Figure 5. Water phantom central-axis depth-dose variations taken for different field sizes in a Co-60 beam, and normalised to the dose delivered by a 10 cm square field at 10 cm depth.

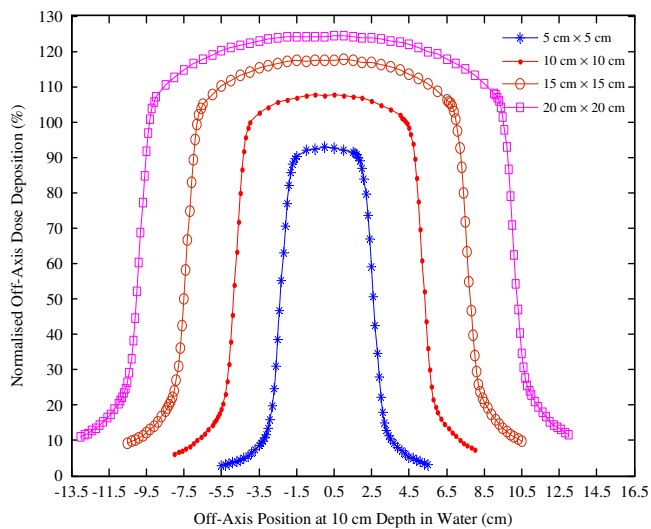


Figure 6. Lateral beam profiles for a clinical MDS Nordion Equinox 80 unit Co-60 beams at 10 cm depth in a water phantom.

collimator jaw motions was investigated by Gafchromic RTQA2-1010 and Gafchromic EBT2 films, respectively. The lateral beam profiles generated from OD_{net} readouts of Gafchromic RTQA2-1010 and Gafchromic EBT2 films²⁰ were analysed to establish beam intensity modulation versus water phantom data. Focus was on the central regions of the lateral beam profiles. Furthermore, DICOM file data for the beam intensity modulation by secondary collimator jaw motions were used concurrently with MC simulations to validate the feasibility of this study.

Film calibration

Figure 7 is a plot of the calibration curves for the Gafchromic EBT2 and RTQA2-1010 films used in this study.^{22,24} Standard errors associated with the calibration per film lot were not visible enough as error bars in the plots.

RTQA2 raw is the calibration data for the RTQA2-1010 film lot, RTQA fit3 is its third-order polynomial curve fit, EBT2 raw is the calibration data for the EBT2 film lot and EBT2 fit3 is the third-order polynomial curve fit to the EBT2 film calibration

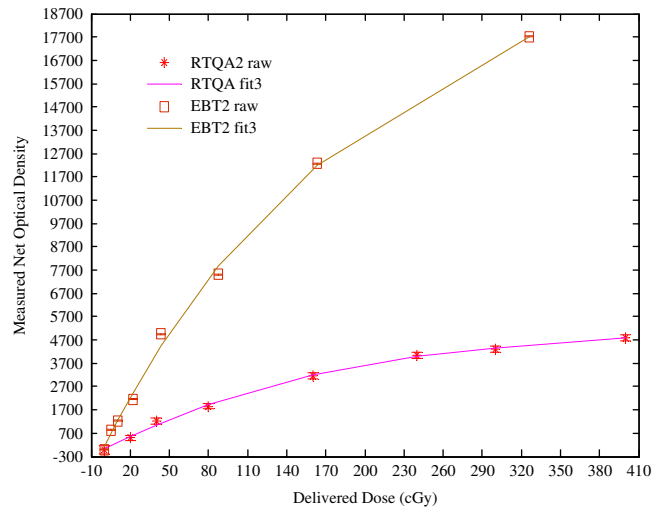


Figure 7. Calibration curves for the Gafchromic EBT2 and RTQA2-1010 films used in this study.

data.^{22,24} The source head fluence of a cobalt-60 teletherapy beam can be effectively modulated by a once-off or fractionated exposure with a 3D physical compensator at the machine source head. Point and planar dosimetry studies performed at 5.0 cm depth and 74.3 cm SSD in a PTW universal IMRT verification phantom using a calibrated batch of Gafchromic RTQA2-1010 film showed that consistent intensity patterns could be obtained with a 3D physical compensator. The MCNPX radiation transport code can be a viable for the treatment planning of the anticipated fluence maps in cobalt-60 teletherapy.

Conclusions

Preferential modulated source head fluences were achieved by sequences of square and rectangular field segments that were symmetric about the axial and sagittal planes. Such field segments were yielded dosimetric characteristics that are comparable to those of linear accelerator beams, more particularly in terms of the penumbral features of the resultant cobalt-60 teletherapy beams. It was further ascertained that Gafchromic EBT2 film OD_{net} data could accurately verify the delivered doses even for the asymmetric field deliveries. Furthermore, in using the same gamma index analysis criteria between Gafchromic EBT2 film measurements and treatment planning system prescriptions, good passing rates were obtained for all cases investigated.

There is a prospect for the resultant cobalt-60 teletherapy source head fluences obtained in this step-and-shoot analogy to span the entire planning target volume, and hence counteract the current penumbra-related dosimetric uncertainties. Results of Gafchromic EBT2 and Gafchromic RTQA2-1010 film measurements showed the viability of radiochromic film as a tool for both point and planar dosimetry in intensity-modulated cobalt-60 teletherapy beams.

Acknowledgements. Special thanks go to Professor Rudolph Nchodu for facilitating a top-up bursary funding from iThemba Labs, without which no meaningful progress would have been made. The Department of Medical Physics at the Charlotte Maxeke Johannesburg Academic Hospital is vastly appreciated for the major role they played with regards to therapy and dosimetry apparatus.

References

- 1 Joshi C P, Dhanesar S, Darko J, Kerr A, Vidyasagar P B, Schreiner L J. Practical and clinical considerations in Cobalt-60 tomotherapy. *J Med Phys* 2009; 34: 137–140.
- 2 Christopher F, Edwin R H, Bart L, Chunhua M, Dionne M A, James F D. Comparative analysis of ⁶⁰Co intensity-modulated radiation therapy. *Phys Med Biol* 2008; 53: 3175–3188.
- 3 Chandra P J, Johnson D, Vidyasagar P B, John S L. Investigation of an efficient source design for Cobalt-60-based tomotherapy using EGSnrc Monte Carlo simulation. *Phys Med Biol* 2008; 53: 575–592.
- 4 Podgorsak E B. *Radiation Oncology Physics Monograph Online*. Vienna: International Atomic Energy Agency, 2005.
- 5 Palta J, Mayles P. editors *Transition from 2-D Radiotherapy to 3-D Conformal and Intensity Modulated Radiotherapy*. Vienna: International Atomic Energy Agency, 2008.
- 6 Fox C, Romeijn H E, Lynch B, Men C, Aleman D M, Dempsey J M. Comparative analysis of ⁶⁰Co intensity-modulated radiation therapy. *Phys Med Biol* 2008; 53 (12): 3175–3178.
- 7 Omer M A A. Partial quality assessment of ⁶⁰Co-teletherapy machine performance. *Open J Radiol* 2015; 5: 235–242.
- 8 Cadman P, Bzdusek K. Co-60 tomotherapy: a treatment planning investigation. *Med Phys* 2011; 38 (2): 556–564.
- 9 Adams E J, Warrington A P. A comparison between cobalt and linear accelerator-based treatment plans for conformal and intensity-modulated radiotherapy. *Br J Radiol* 2008; 81: 304–310.
- 10 Rachivandran R. Has the time come for doing away with cobalt-60 teletherapy for cancer treatments? *J Med Phys* 2009; 34: 63–65.
- 11 Bucci M K, Bevan A, Roach M. Advances in radiation therapy: conventional to 3D, to IMRT, to 4D, and beyond. *CA Cancer J Clin* 2005; 55: 117–134.
- 12 Van der Molen L, Heemsbergen W D, de Jong R et al. Dysphagia and trismus after concomitant chemo-intensity-modulated radiation therapy (chemo-IMRT) in advanced head and neck cancer; dose-effect relationships for swallowing and mastication structures. *Radiother Oncol* 2013; 106 (3): 364–369.
- 13 Kerr A, Rawluk N, MacDonald A, Marsh M, Schreiner J, Darko J. Cobalt-60 source based image guidance on broad beam cobalt-60 IMRT. *Int J Radiat Oncol Biol Phys* 2010; 78 (3): S701.
- 14 Sumia E M E, Mustafa M E. (2008). Evaluation of motorized wedge for a new generation telecobalt machine, Sudan Academy of Sciences, Atomic Energy Council.
- 15 Eeva K S, Krystyna K, Geoffrey S I et al. International conference on advances in radiation oncology (ICARO): outcomes of an IAEA meeting. *Radiat Oncol* 2011; 6: 11.
- 16 Welsh J S, Mackie T R, Limmer J P. High-energy photons in IMRT: uncertainties and risks for questionable gain. *Technol Cancer Res Treat* 2007; 6 (2): 147–149.
- 17 Das I J, Ding G X, Ahnesjo A. Small fields: nonequilibrium radiation dosimetry. *Med Phys* 2008; 35 (1): 206–215.
- 18 Vicini F A, Kini V R, Edmundson G, Gustafson G S, Stromberg J, Martinez A A. A comprehensive review of prostate cancer brachytherapy: defining an optimal technique. *Int J Radiat Oncol Biol Phys* 1999; 44: 483–491.
- 19 Yuichi A, John P G, Daniel W N, Connel C, Indra J D. Intra- and intervariability in beam data commissioning among water phantom scanning systems. *J Appl Clin Med Phys* 2014; 15 (4): 251–258.
- 20 Satish C U, Umesh C N, Sunil D S. Evaluation of Gafchromic EBT2 film for the measurement of anisotropy function for high-dose-rate ¹⁹²Ir brachytherapy source with respect to thermoluminescent dosimetry. *Rep Pract Oncol Radiother* 2011; 16 (1): 14–20.
- 21 Daniel L. The importance of 3D dosimetry. *J Phys Conf Ser* 2015; 573: 012009 <https://doi.org/10.1088/1742-6596/573/1/012009>.
- 22 Devic S. Radiochromic film dosimetry: past, present, and future. *Ystad, Sweden: Elsevier Ltd*, 2010; 27: 122–34 <https://doi.org/10.1016/j.emp.2010.10.001>.
- 23 Girard F, Bouchard H, Lacroix F. Reference dosimetry using radiochromic film. *J Appl Clin Med Phys* 2012; 13 (6): 1–12.
- 24 Girard F, Bouchard H, Lacroix F. Reference dosimetry using radiochromic film. *J Appl Clin Med Phys* 2012; 13 (6): 339–353 <https://doi.org/10.1120/jacmp.v13i6.3994>.